JAAS

Accepted Manuscript

This is an *Accepted Manuscript*, which has been through the Royal Society of Chemistry peer review process and has been accepted for publication.

Accepted Manuscripts are published online shortly after acceptance, before technical editing, formatting and proof reading. Using this free service, authors can make their results available to the community, in citable form, before we publish the edited article. We will replace this *Accepted Manuscript* with the edited and formatted *Advance Article* as soon as it is available.

You can find more information about *Accepted Manuscripts* in the Information for Authors.

Please note that technical editing may introduce minor changes to the text and/or graphics, which may alter content. The journal's standard Terms & Conditions and the Ethical guidelines still apply. In no event shall the Royal Society of Chemistry be held responsible for any errors or omissions in this *Accepted Manuscript* or any consequences arising from the use of any information it contains.

ROYAL SOCIETY OF CHEMISTRY

www.rsc.org/jaas

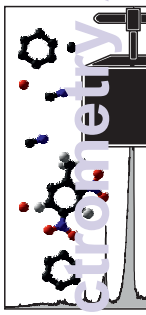

PRIMARY AND RECOMBINED EMITTING SPECIES IN LASER-INDUCED PLASMAS OF ORGANIC EXPLOSIVES IN CONTROLLED ATMOSPHERES

Tomás Delgado, José M. Vadillo and J. Javier Laserna*

Universidad de Málaga, Departamento de Química Analítica, 29071 Málaga, España

ABSTRACT

The main difficulties in spectral interpretation of laser-induced plasmas from species containing C, N, O or H relies on the crossroad concerning their origin: direct release from native bonds of the molecule or recombination of atoms and molecular fragments with ambient constituents. In order to add further insight to the issue, this paper presents the influence of the surrounding ambient (gas type and pressure) on the spectra of energetic nitro compounds (TNT and PETN). The study was completed with coincidental detection at high vacuum of both optical emission and mass spectra originated from the same laser event. We have proposed probable fragmentation pathways for the compounds taking into account the reactions that prevail over other routes depending on experimental conditions: laser fluence, pressure and surrounding atmosphere. The suggested routes are supported by identification of many non-emitting, reactive species present in the plasma using the corresponding mass spectra.

Keywords: Laser induced breakdown spectroscopy, Laser ionization mass spectrometry, ion-photon detection, energetic compounds, molecular emission

1. Introduction

Laser plasmas are an extremely reactive chemical environment where atoms, molecules, ions and electrons interact in rather favourable thermodynamic conditions due to their high electron density and elevated electronic temperatures. The extension of such reactions may be substantially as the experimental conditions change, particularly the surrounding media.

The large majority of laser-induced breakdown spectrometry (LIBS) experiments are performed on metals in air at atmospheric pressure, where recombination mechanisms do not play a significant role, as the primary emission lines of interest are significantly more intense than those derived from recombination with air, particularly those yielding oxides.[1,2] Due to the large number of electronic transitions commonly attainable as a result of LIBS on metals, many intense emission lines are recorded and different regions of interest useful for identification and quantification purposes may be assigned.

The main difficulties in the interpretation of the molecular emission of species containing C, N, O or H relies on the questions concerning their origin: direct release from native bonds or recombination with ambient constituents. In other words: does the LIBS spectrum mimic the structure of a molecule or the molecular information gets lost in the course of the secondary reactions? Considering that the spectrum observed is always a convolution of primary and secondary processes, experiments in vacuum or in controlled atmospheres may help to address such questions.

An important problem that has to be faced concerns the lack of temporal or spatial homogeneity in the expanding plasma.[3,4] Consequently, any attempt to establish general assumptions over the whole plasma extracted from specific spatial locations or at narrow temporal windows are quite risky. On the other hand, LIBS information relies exclusively on emitting neutral or ionized states, whereas other particles formed (polyatomic neutrals and ions) are usually not detected. The authors have previously used mass spectrometry combined with optical emission spectroscopy in the characterization of laser-induced plasmas.[5] Initially, the idea of combining ion

and photon detection in the same setup seems appealing as it provides orthogonal information from the system. From the experimental point of view, ion and photon detection from laser-produced plasmas differ quite significantly, not only due to the high-vacuum conditions required in mass spectrometry, but also because of the limited tolerance of mass spectrometers to deal with highly energetic ions. Thus, the ideal conditions for mass spectrometry are very close to the plasma formation threshold where the less energetic ions are easier to focus, and the output yields mass spectra with lower fragmentation. Under such conditions, optical emission is largely reduced, close to the sensitivity limit of any practical optical detection scheme. The main shortcoming of mass spectrometry in comparison to optical emission relies on the lack of temporal discrimination in the measurements. As the mass spectrum represents a time-integrated view of the ions present in the plasma, we have adjusted the acquisition parameter of LIBS to those of our LIMS setup, as commented in the experimental section.

The present work is based on pressure-controlled experiments performed over an eight orders of magnitude range in air (from atmospheric to 10^{-5} mbar) as well as under controlled H_2 and N_2 atmospheres. In the pressure range between 10^{-4} to 10^{-6} mbar, we performed simultaneous LIMS-LIBS detection. From a spectrochemical point of view, modifications of the expanding media have a direct reflection in the emission intensity, and it is expected a similar trend in all the species formed simultaneously in a laser plasma. However, the following of the different species present in our expanding plasmas as a function of base pressure has demonstrated three different behaviours, with different species exhibiting intensity maxima at different pressures ranges. This fact indicates the coexistence of different processes and a much more complex explanation for the results than just a better free expansion of the plasma.

Two compounds, 2,4,6-trinitrotoluene (TNT, $C_7H_4N_3O_6$) and pentaerythritoltetranitrate (PETN, $C_4H_8N_4O_{12}$) were selected for the study. Both compounds have NO_2 groups in their structure as a native source of N, whereas only TNT is aromatic and has carbon-carbon double bonds. Apart from the interest in the active field of forensic LIBS,[6-14] a better knowledge about

thermal decomposition mechanisms are fundamentally important in the explosives field and the determination of the kinetics and reactions of this breakdown process remains a fundamental aspect of their characterization.[15,16] Pyrene has been used as a control aromatic chemical system due to the absence of N or O in its structure.

2. Experimental

A scheme of the experimental set-up is shown in Figure 1. For this study, a quadrupled Nd:YAG laser (266nm, 5 ns pulse width) was used to irradiate the samples, located in the ionization chamber of a time-of-flight (TOF) mass spectrometer. Pressure in the chamber was monitored in the 10^{-4} to 10^{3} mbar range by a Pirani gauge and an ionization gauge was used to control vacuum pressure into the time-of-flight analyzer. Buffer gases were introduced in the chamber through a needle valve. The chamber was entirely isolated and a purge system with Ar was installed to remove the buffer gas after finishing each analysis. After a purge cycle, turbo molecular pumps were switched on to ensure complete evacuation of the system. Laser pulse energy was controlled using a variable attenuator that allowed continuous variation of the energy without modifications in the beam spatial profile. The laser beam was focused on the sample surface with a 25 mm quartz plane-convex lens (f = 200 mm) leading to a spot size of 2.77 x 10^{-4} cm^2. Light emitted from the plasma plume (from the nearest location to the sample surface) was 1:1 focused by a 75 mm quartz planoconvex lens (f = 150 mm) onto a quartz optical fibre (1 mm diameter) placed orthogonal to the plume expansion direction and connected to the entrance slit of a 0.5 m focal length spectrograph (F/6.5) fitted to a gated ICCD detector. A 600 grooves/mm grating allowed a dispersion of 0.13 nm/pixel and a spectral coverage of 40 nm. Full spectral range acquisitions at different pressure levels were automatically obtained by successive measurements performed on overlapping 20 spectral windows (each one consisting of 30 accumulated spectra in order to reach satisfactory signal-to-noise ratio). For the study of the evolution of emission signals with pressure for each species of interest, independent series of 100 accumulated spectra were taken using the corresponding spectral window. The sample surface was continuously refreshed to avoid bias in the data as a result of different ablation conditions.

Ion fragments from the sample were extracted and accelerated in an orthogonal geometry. During mass analysis, a minimum pressure difference of one order of magnitude was kept between the ionization chamber and the flight tube by differentially pumping. A minimum pressure of 10^{-5}

mbar was always kept in the ionization chamber to assure safe operation of the detector, whose output was sent to a 500-MHz digital storage oscilloscope. Series of 600 mass spectra (associated to 600 laser events) were acquired for every coincidence measurement. The electronic configuration of the system allowed the detection of positive ions only. Both LIBS and LIMS systems were synchronized by means of a pulse and delay generator (PDG). The trigger signal from the laser reached the PDG and it let both the extraction electrode and ICCD camera aperture at the same time so that temporal parameters of signal acquisition were matched. The delay between the laser firing and the starting of the detection cycles in the ICCD and TOF was set at 50 ns to capture all the events since early moments. Smaller delays yielded broad optical spectra with negligible information. Unless specified, a 1 ms acquisition window was used for photons detection to assure the recording of whole plasma emission. For TOF, the deflection pulse for the orthogonal extraction was set to 800 ns.

2,4,6-TNT and PETN samples were obtained from the Laboratorio Químico Central de Armamento of the Ministry of Defence and prepared by compressing bulk powders using a hydraulic press machine to obtain 10 mm in diameter and 2 mm thick pellets. Samples were then placed onto an aluminium holder that was introduced into the auxiliary chamber for primary vacuum by means of an insertion probe equipped with a 3D micrometer for fine control of the position of the sample. This handler was finally introduced in the main chamber through a typical gate valve to place the sample in the final location.

3. Results and Discussion

Pressure-controlled experiments allow a precise monitoring of the species formed in laser-induced plasmas under variable expanding conditions. Using identical excitation parameters, differences observed in emission intensities correspond to variations in the ablation behaviour as the expansion occurs in atmospheres differing largely in presure. Figure 2 shows the typical emission spectrum of TNT resulting from ablation under identical conditions in vacuum (top) and in air at atmospheric pressure (bottom). The spectra were acquired from close-to-surface positions with a delay of 50 ns after the laser firing and were integrated over the time (integration time >1 ms). Under these conditions, the background is significant in the spectra. Such unfavourable conditions for detection of neutral signals allow a quite good evidence of the effect of lowering the base pressure on the reduction of background. The laser fluence was chosen to provide large signal-to-noise ratio (SNR) in the atomic lines and molecular bands with reduced sample damage. The spectra have been plotted to the same intensity scale with an offset. As observed, the LIBS spectrum in air at atmospheric pressure is dominated by emissions from the C_2 Swan system and the CN Violet system with weak (if detectable) signals from atomic species. However, the spectrum in vacuum is dominated by atomic and ionic emissions with much lower contribution from diatomic species. Initially, the significant reduction in the CN signal in vacuum might be directly attributed to the complete removal of atmospheric N_2 from the surrounding gas, impairing the formation of CN molecules. However, this fact does not explain the drop in vacuum of the C_2 signal as the only source of C is the sample itself.

Electron density (n_e) and electronic temperature (T_e) were computed to correlate their variation in the pressure range studied with the differences observed in the emitting species. Under our experimental conditions, calculation of temperature can be done with reasonable precision for pressures below 0.1 mbar, the only pressure range where the H_α, H_β and H_γ were simultaneously visible over the background. In such range, the electron temperature averaged 13000 ± 2000 K. For pressures over 1 mbar only H_α was visible. Concerning n_e, it was not estimated as it depends on T_e

for the calculation of the electron impact width parameter included in its expression. However, as the H_α is visible, it is possible to plot the FWHM of the H_α line as a function of the base pressure. These results are shown in Figure 3. As observed, a sharp increase in line width occurs from 1 mbar. In the plateau region, based on the calculated temperature with the Boltzmann plot using the H_α, H_β and H_γ lines, the electron density has a value of 5.0×10^{16} cm^{-3}, indicating local thermodynamic equilibrium according to the McWhirter criterion. Such value, due to the uncertainty in the measurements for the short delay time used, must be used as an indication and not as an absolute value.[17,18] On the other hand, in a transient plasma as ours, the McWhirter criterion is not enough to ensure LTE and the calculation of the optical time-of-flight for the chemical species in the plasma and the variation length of temperature and electron density along the plasma expansion axis[19] is not achievable with our collection setup.

The relative abundance of the species present in the plasma under different vacuum levels exhibits a complex behaviour. Figure 4 shows the net peak intensities of N, O, C, H, CN and C_2 for TNT as a function of pressure in the interval between 10^3 and 10^{-4} mbar. The experimental conditions to perform the experiment started at 10^{-4} mbar. Once recorded the data, air was leaked into the chamber through a needle valve until a desired pressure was reached. The operation was repeated until reaching atmospheric pressure. Each data set, corresponding to the evolution of a single species, is represented at their maximum intensity. Although the signals are only relative intensities and cannot be considered as absolute representations of the species abundance, the plot serves for comparative purposes. As shown, CN and C_2 exhibit largest intensities in the range between 10-100 mbar. Their intensities drop markedly below 1-10 mbar. For pressure values lower than 0.1 mbar, their presence in the spectra is significantly reduced, although not completely extinguished, as it can be seen in Figure 5 (top), where even at pressures of 10^{-4} mbar, the intensity of the CN Violet system is quite significant.

The different pathways for CN formation have been discussed in the literature,[4,6,19-23] and can be summarized as follows:

$$C + N_2 \rightleftharpoons CN + N \quad (1)$$

$$C_2 + N_2 \rightleftharpoons 2CN \quad (2)$$

$$CH_n + N \rightleftharpoons CN + CH_{n-1} \quad (3)$$

$$[TNT] \longrightarrow nCN + mC_2 + \text{other prod.} \quad (4)$$

$$C + NO \rightleftharpoons CN + O \quad (5)$$

In the presence of atmospheric N_2, reactions (1) and (2) are obvious. However, the significant presence of CN signals even at 10^{-4} mbar (as shown in Figure 5) can´t be explained according to these routes. This fact supports the hypothesis of the existence of secondary sources of CN. The first one (a variation of reaction (1) where the precursors are in atomic form) is the two-body recombination process of C atoms with N atoms (C + N → CN) as well as recombination of N with fragments from the dissociation of the aromatic ring (3). Also, reaction of C with NO fragments could lead to CN radicals (5). In the two last reactions, the products (NO and CH_n) are not detected in the optical emission spectra but are easily identified in a mass spectrum (as will be further commented), thus confirming the possibility of reactions (3) and (5).

A second source of CN comes from the direct emission of native CN bonds (4) that become only noticeable when the molecule itself is the only source of N. Experiments performed with TNT under different fluence conditions[24] have shown the existence of CN emission at fluence values lower than those required to get emission from N, C, O or H. This observation would support pathway (4). However, this route based on the release of CN from the molecule should be clearly less significant than route (5), based on the most favourable release of the NO_2 groups.[5] Again, the evidence provided by mass spectrometry on the presence of C^+ and NO^+ in our measurements[25] supports this alternative route.

In order to confirm the feasibility of reaction (4) in the gas-phase chemistry of the TNT, similar experiments were performed with pyrene. This molecule was studied due to the absence of N in its structure. Thus, spectral emission of the pyrene plasma at low pressure can provide suitable information on this issue. Figure 5b sketches the emission spectra of pyrene at different pressure

values. In the pressure range plotted, the largest intensity is observed at 1 mbar. At lower pressures, CN emission is reduced drastically due to the lack of the reactive species. Only when the sample itself acts as the N source (as it occurs with TNT in Figure 5a) CN emission will be visible at low pressure. Thus, it seems clear that pathway (4) occurs during laser ablation of TNT, without precluding the two body reaction mentioned above. A deeper comparison between laser-induced plasma plumes of both compounds and the consequent emission signals was presented in a previous work.[26]

In the case of C_2 emissions, the presence of double or triple carbon-carbon bonds is required,[20,27] and several formation pathways are also possible: either from direct fragmentation of the aromatic ring of the parent compound according to reaction (4) or from reaction (6) between resulting hydrocarbon radicals present in the plasma.[28]

$$CH_n + CH_m \rightleftharpoons C_2 + (n + m)H \qquad (6)$$

Moreover, C-C recombination in the hot plasma is also possible.[22,29] In any of the probable reactions, ring opening and fragmentation is required. Thus, any modification in the stability of the ring modifies the C_2 emission.[27] This fact has been experimentally demonstrated in the homologous series of nitrotoluenes, where the C_2 emission decreased with the number of inductive and resonance electron-withdrawing NO_2 groups.[6]

The trend of C and C_2 in Figure 3 follows an opposite pattern, the C signals being less intense in the mid-high pressure region where C_2 emission is larger. This fact suggests a direct correlation between release and consumption of such species through different routes. In this point, mass spectrometry represents a valuable tool due to its capability for monitoring the C_nH_m resulting from aromatic ring opening. While in high vacuum, the optical emission spectrum (Figure 6 top) reveals emission signals mainly from atomic/ionic species, the presence of C_nH_m species from ring fragmentation becomes evident in the mass spectra acquired simultaneously as shown in Figure 6 (bottom). Indeed, the ion fragments from $^{13}CH^+$ to $^{50}C_4H_2^+$ are clearly identified. The presence of electrons in the plasma is responsible of the final electron-impact dissociation of C_nH_m fragments to

C and H as it occurs in similar techniques where it occurs the fragmentation of organics by means of released electrons from surfaces or plasmas occurs.[30,31] The concomitant release of C and H formed in the dissociation of C_nH_m explains the increased abundance of atomic species in the plasma and the subsequent enhancement of their emission intensities in the high-vacuum regime noticed in Figure 3. In this high-vacuum region, the spectral width of our emission lines remains constant (see Figure 2) and in principle, it could be assumed that the described intensity variations are not related to significant changes in the plasma conditions.

The absence of significant CN and C_2 emissions observed in Figure 6 is believed to be due to two interesting reactions (9,10) that involve their recombination with H_2:

$$C_2 + H \rightleftharpoons CH + C \qquad (7)$$

$$CN + H_2 \rightleftharpoons HCN + H \qquad (8)$$

These routes might be partially responsible of the reduction of molecular emissions observed in vacuum. The presence of H_2 in vacuum would be due to the CH_n radical that by ladder switching would release potentially reactive atomic species involved in the reactions described above:

$$CH_n \rightleftharpoons CH_{n-1} + H \qquad (9)$$

Again, mass spectrometry helps to clarify such reactions as signals at fragments $^{13}CH^+$ and $^{28}HCNH^+$ are evident in Figure 6.

The trend of N_2 and O_2 in Figure 3 is quite similar, their intensities increasing from 1000 mbar and yield a clear maximum at 1 mbar. From this point, their intensities fall again in the higher vacuum region. The maximum intensity observed at intermediate pressures is not fully explained and is most probably due to a combination of factors with the permanent presence of NO released from NO_2 of the aromatic ring. As the pressure decreases, the electrons responsible of the NO dissociation may operate more efficiently, reaching the maximum at 1 mbar. From this point, competitive reactions (as those yielding NH and OH as discussed below) consume the N and O in the surroundings, thus decreasing their emission intensity.

Such pool of different reactions indicates the complexity of the laser-matter interaction even with molecules of simple composition as the organics considered, and highlights the evidence of the final LIBS spectra resembling the molecular structure of the ablated sample. To check this point, TNT (Figure 6) and PETN (Figure 7) are compared under identical conditions in our simultaneous ion-photon detection scheme.

Figure 6 shows the TNT LIBS (top) and LIMS (bottom) averaged spectra at 3.6 J/cm^2. Such fluence value is slightly above the plasma formation threshold. Under these soft conditions, the LIBS spectrum shows contributions from CN and C_2, and evidences of C, H and O. The presence of the ions $^{12}C^+$, $^{13}CH^+$, $^{24}C_2^+$, $^{26}C_2H_2^+$,$^{28}CO^+$/$^{28}HCNH^+$ in the mass spectrum supports the reactions commented in previous paragraphs as possible routes of dissociation. The presence of carbon is probably distributed in different C-based fragments due to the break of the aromatic ring:

$$\Sigma C = {}^{12}C^+ + {}^{24}C_2^+ + \Sigma C_nH_m^+ \qquad (10)$$

Ring-opening is demonstrated based on the appearance in the mass spectrum of multiple signals associated to the ladder-switching process associated to the presence of aromatics, and compatible with reaction (9). The ion signal at m/z=28$^+$ is attributed to CO^+, which supports the evidence of consumption of C_2 and O through reaction (11).

$$C_2 + O \rightleftharpoons CO + C \qquad (11)$$

Thus, H and O present in the plume since the first nanoseconds of plasma lifetime could prevent the observation of molecular fragments signals according to reactions (7), (8) and (11) under vacuum conditions. On the contrary, at atmospheric pressure, reactions from (1) to (3) take place predominantly under the action of N_2 gas and molecular bands from CN and C_2 fragments dominate the spectrum.

The mass spectrum was dominated by the $^{30}NO^+$ ion derived from the immediate dissociation of NO_2 groups that were rapidly ejected from aromatic ring due to the stress of the molecule caused by the position of substituents in the space. The nitro explosives had a common feature, namely a relatively high degree of charge separation, and in the proposed energetic

molecules, the presence of NO_2 group introduced significant charge separation or local polarity. The nitro group is powerfully electron-attracting and this fact strongly conditioned the fragmentation routes followed by the molecules.[32]

PETN was also subjected to simultaneous ion-photon experiments (Figure 7). In the LIBS spectrum (top) it is remarkable the absence of C_2 emissions, expected due to the lack of C=C bonds in the molecule. On the other hand, molecular CN fragments are evident. Taking as reference the acquired LIMS spectrum (bottom), the main reactions suggested in the fragmentation of PETN in vacuum regime were mentioned above, namely (3), (5) and (8). In this case, direct fragmentation of CN radicals from the molecule is not possible since C-N bonds are not present in the structure. Thus, CN fragments are mostly formed in reactions of atomic N_2 with carbon-containing species (3). Also, secondary reactions as (5) are possible. On the other hand, CN radicals could react with traces of H_2 (8) and water (12) molecules in the surrounding to result in a new dissociation, keeping the CN balance in the plume.

$$CN + H_2O \rightleftharpoons HCN + OH \qquad (12)$$

Again, the LIMS spectrum demonstrates the presence in the plasma of the species involved in the shown reactions. The presence of the ions $^{12}C^+$, $^{13}CH^+$, $^{17}OH^+$,$^{18}H_2O^+$, $^{28}CO^+$/$^{28}HCNH^+$, and $^{30}NO^+$ was confirmed. These observations support the decomposition pathways proposed for this compound. Characteristic hydrocarbon fragments from ladder-switching reaction associated to the presence of benzene cycles are absent. Moreover, total fragmentation or atomization of PETN was found to occur at fluence higher than that needed for TNT. This fact may be related to the molecular stability of PETN and, therefore, the spatial distribution of substituents that makes the structure to be less stressed than in the case of TNT system.

Hydrogen and nitrogen atmospheres

The hypothesis of consumption of C_2 and CN species at vacuum ambient by H_2 after reactions (7) and (8) is supported by an experiment using H_2 as buffer gas. If such reactions would

proceed to a significant extent in the plasma, measurements in a H_2 atmosphere would result in an increase in the intensity of CH and a depletion of the C_2 and CN emissions. In the experiment, H_2 from a gas cylinder was allowed to leak into the vacuum chamber and plasma light was collected at different background pressure levels from high vacuum to 3.5 mbar (top pressure of the calibrated range for H_2 gas). Figure 8 compares the LIBS spectra of TNT acquired in N_2 and H_2 atmospheres at 1 mbar. Both spectra are plotted to the same scale. In the case of N_2 as buffer gas, intense CN and C_2 molecular bands are evident. Also notable is the presence of the emission system corresponding to NH at 336.0 nm and 337.0 nm. The increase of emission intensity for excited NH was appreciable compared to that obtained for other background atmospheres due to a larger rate of association between N_2 from background gas and H atoms.

In contrast, the H_2 atmosphere yields an increased CH band, whereas the intensity of the CN and C_2 emissions decreases dramatically. This result was similar to that obtained in high vacuum pressure conditions. In vacuum, CN and C_2 arise from the direct rupture of the aromatic ring since only a low degree of recombination was possible. The velocity of plasma expansion is quite high and this involves the virtual absence of collisional processes in the plume. However, when H_2 was present as background gas, the number of collisions inside the plasma increase gradually. In fact, a strong broadening effect was observed for emission lines of atomic H_α and H_β at pressures above 3.5 mbar due to the higher electronic density of the plasma. After such evidences, it is possible to conclude that routes (7) and (8) play an important role in the chemistry of the plasma.

The measurement in a N_2 atmosphere also suggests that reaction (2) is only of marginal relevance in the formation of CN. Indeed the spectrum in Figure 8 shows that the abundance of C_2 in the plasma is larger in N_2 atmosphere, which would not be the case if reaction (2) proceeds to a significant extent. The low probability of this reaction pathway in laser-induced plasmas has been predicted in previous reports.[23]

Within the studied pressure range from 0.1 mbar to 3.5 mbar for H_2 atmosphere, different diatomic emitting species, namely CH, NH and OH, were also visible. Figure 9 shows the compared spectra

for TNT and PETN. Both spectra are to scale. We can expect that H_2 from buffer gas leads to the formation of these emitting species in a considerable extent. Formation of CH could mainly follow routes (7) and (9) for both compounds according to the observed LIMS spectra. On the other hand, recombination of NH would follow the route below (13) whereas OH fragments mostly appear from pathway (12) and reactions between atoms in the functional groups inside the own molecule. It is noteworthy how such H-containing fragments exhibit comparable intensities to those for the CN emission at 388 nm in presence of H_2 buffer gas.

$$N + H_2 \rightleftharpoons NH + H \qquad (13)$$

4. Conclusions

In the present work we have collected and characterized LIBS spectra of TNT and PETN, two organic nitro-containing compounds. We have proposed probable fragmentation pathways for the compounds taking into account the reactions that prevail over others depending on experimental conditions: laser fluence, pressure and surrounding atmosphere. The suggested routes are supported by LIMS measurements where many non-emitting, reactive species present in the plasma were identified.

Pressure becomes a critical parameter in LIBS trials affecting the dynamics of the plasma from values as little as 0.1 mbar. Results obtained in N_2 and air atmospheres indicate that C_2 emission is strongly linked to molecular structure whereas CN is mostly produced by chemical reactions. Results in a H_2 atmosphere strongly suggest that H_2 may alter the formation pathways for molecular species, thus reducing the CN and C_2 emissions, while favouring the formation of NH, CH and OH. We have verified this effect in absence of air, where molecular emission was also very weak. This fact is presumably caused by the reaction of H_2 mostly and other atomic species with molecular species inside the plasma resulting in dissociation of such fragments (CN, C_2…).

Acknowledgments

We gratefully acknowledge financial support for this work by Consejería de Innovación, Ciencia y Empresa de la Junta de Andalucía (Project P07-FQM-03308). This work was also partially supported by Ministerio de Economía y Competitividad (Projects CTQ2008-02197 and CTQ2011-24433).

References

[1] A.L. Lewis and E. H. Piepmeier, *Appl. Spectrosc.,* 1983, **37**, 523-530.

[2] G. J. Beenen and E. H. Piepmeier, *Appl. Spectrosc.* 38 (1984) 851-857.

[3] S. Grégoire, V. Motto-Ros, Q. L. Ma, W. Q. Lei, X. C. Wang, F. Pelascini, F. Surma, V. Detalle and J. Yu, *Spectrochim. Acta, Part B*, 2012, **74-75**, 31–37.

[4] M. Baudelet, M. Boueri, J. Yu, S. S. Mao, V. Piscitelli, X. Mao and R. E. Russo, *Spectrochim. Acta, Part B*, 2007, **62**, 1329-1334.

[5] J. M. Vadillo, C. C. Garcia, J. F. Alcántara, J. J. Laserna, *Spectrochim. Acta, Part B*, 2005, **60**, 948–954.

[6] P. Lucena, A. Doña, L. M. Tobaria and J. J. Laserna, *Spectrochim. Acta, Part B*, 2011, **66**, 12–20.

[7] C. Mullen, A. Irwin, B. V. Pond, D. L. Huestis, M. J. Coggiola and H. Oser, *Anal. Chem.*, 2006, **78**, 3807-3814.

[8] J. L. Gottfried, F. C. De Lucia Jr., C. A. Munson and A. W. Miziolek, *J. Anal. At. Spectrom.*, 2008, **23**, 205–216.

[9] J. Moros, J. A. Lorenzo, P. Lucena, L. M. Tobaria and J. J. Laserna, *Spectrosc. Eur.*, 2010, **22**, 18-22.

[10] R. González, P. Lucena, L.M. Tobaria and J. J. Laserna, *J. Anal. At. Spectrom.*, 2009, **24**, 1123-1126.

[11] J. Moros, J. A. Lorenzo, P. Lucena, L. M. Tobaria and J. J. Laserna, *Anal. Chem.*, 2010, **82**, 1389-1400.

[12] M. Abdelhamid, F. J. Fortes, M. A. Harith and J. J. Laserna, *J. Anal. At. Spectrom.* 2011, **26**, 1445-1450.

[13] J. Moros, J. A. Lorenzo and J. J. Laserna, *Anal. Bioanal. Chem.*, 2011, **400**, 3353 - 3365.

[14] J. Moros and J. J. Laserna, *Anal. Chem.*, 2011, **83**, 6275 - 6285.

[15] G. F. Adams and R. W. Shaw, *Annual Rev. of Phys. Chem.*, 1992, **43**, 311-340.

[16] R. Cohen, Y. Zeiri, E. Wurzberg and R. Kosloff, *J. Phys. Chem. A*, 2007, **111**, 11074-11083.

[17] N. Farid, S. S. Harilal, H. Ding and A. Hassanein, *J. Appl. Phys.*, 2014, **115**, 0331071-0331079.

[18] J. R. Freeman, S. S. Harilal, P. K. Diwakar, B. Verhoff and A. Hassanein, *Spectrochim. Acta*, 2013, **87**, 43–50.

[19] G. Cristoforetti, A. De Giacomo, M. Dell'Aglio, S. Legnaioli, E. Tognoni, V. Palleschi and N. Omenetto, *Spectrochim. Acta, Part B*, 2010, **65**, 86–95.

[20] L. St-Onge, R. Sing, S. Béchard and M. Sabsabi, *Appl. Phys. A*, 1999, **69**, S913-S916.

[21] A. Portnov, S. Rosenwaks and I. Bar, *Appl. Opt.* 2003, **42**, 2835–2842.

[22] A. Kushwaha, R. K. Thareja, *Appl. Opt.,* 2008, **47**, G65-G71.

[23] Q. Ma and P. J. Dagdigian, *Anal. Bional. Chem.*, 2011, **400**, 3193-3205.

[24] T. Delgado, J. Vadillo and J. J. Laserna, *J. Anal. At. Spectrom.* 2013, **28**, 1377-1384.

[25] T. Delgado, J. F. Alcantara, J. Vadillo and J. J. Laserna, *Rapid Commun. Mass Spectrom.* 2013, **27**, 1807-1813.

[26] T. Delgado, J. Vadillo and J. J. Laserna, *Appl. Spectrosc.*, 2014, **68**, 33 - 38.

[27] A. Portnov, S. Rosenwaks and I. Bar, *J. Lumin.*, 2003, **102-103**, 408-413.

[28] K. Sovova, K. Dryahina, P. Spanel, M. Kyncl and S. Civis, *Analyst*, 2010, **135**, 1106-1114.

[29] Z. Zelinger, M. Novotny, J. Bulir, J. Lancok, P. Kubat and M. Jelinek, *Contrib. Plasma Phys.*, 2003, **43**, 426-432.

[30] B. W. LaFranchi and G. A. Petrucci, *Int. J. Mass Spectrom. Ion Proc.*, 2006, **258**, 120-133.

[31] P. Y. Cheng and H. L. Dai, *Rev. Sci. Instrum.*, 1993, **64**, 2211-2214.

[32] J. S. Murray, P. Lane and P. Politzer, *Mol. Phys.*, 1998, **93**, 187-194.

Figures

Figure 1. Schematic diagram of experimental setup for LIBS-LIMS spectra acquisition.

Figure 2. LIBS broadband spectra of TNT acquired at two different pressures: (Top) $1.0x10^{-4}$mbar, (Bottom) 1000 mbar. Delay time: 50 ns; acquisition time: 1 ms. Laser wavelength: 266 nm. Energy per pulse: 3.5 mJ (Fluence: 12.6 J /cm^2).

Figure 3. Evolution of FWHM of the Hα line as a function of pressure for a TNT sample. The shadowed region indicates the range where H_α, H_β and H_γ are visible and electronic temperature was calculated.

Figure 4. Net intensities of main emitting species from respective emission spectra as a function of pressure level. Acquisition conditions as in Figure 2.

Figure 5 Detail of CN emission spectra for TNT (top) and pyrene (bottom) samples at different base pressures. Acquisition conditions as in Figure 2.

Figure 6. Simultaneous LIBS (top) and LIMS (bottom) spectra of TNT. Pressure: 10^{-5} mbar. Excitation: 266 nm. Energy per pulse: 1 mJ (Fluence, 3.6 J /cm^2). LIBS conditions: 50 ns delay time; 1 ms acquisition time. LIMS conditions: 800 ns extraction pulse.

Figure 7. Simultaneous LIBS (top) and LIMS (bottom) spectra of PETN. Pressure: 10-5 mbar. Excitation: 266 nm. Energy per pulse: 2 mJ (Fluence, 7.2 J /cm^2). LIBS conditions: 50 ns delay time; 1 ms acquisition time. LIMS conditions: 800 ns extraction pulse.

Figure 8. LIBS spectra of TNT acquired in rarefied H_2 and N_2 atmospheres at a base pressure of 1 mbar. Acquisition conditions as in Figure 2.

Figure 9. Detailed LIBS spectra (300-440 nm spectral range) of PETN (solid line) and PETN (shadowed) in a rarefied H_2 atmosphere at a base pressure of 3.5 mbar. (H_2 atmosphere at 3.5 mb for (a) TNT and (b) PETN. Acquisition conditions as in Figure 2.

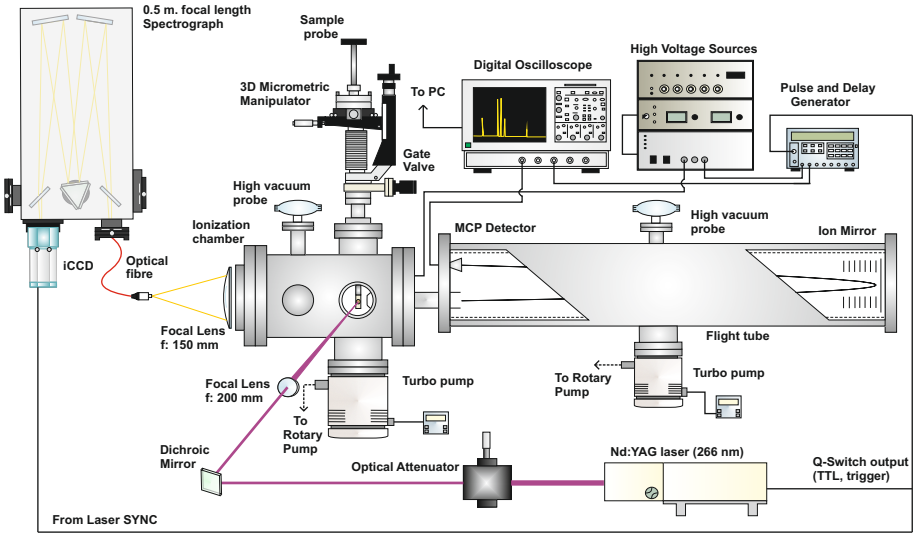

Figure 1

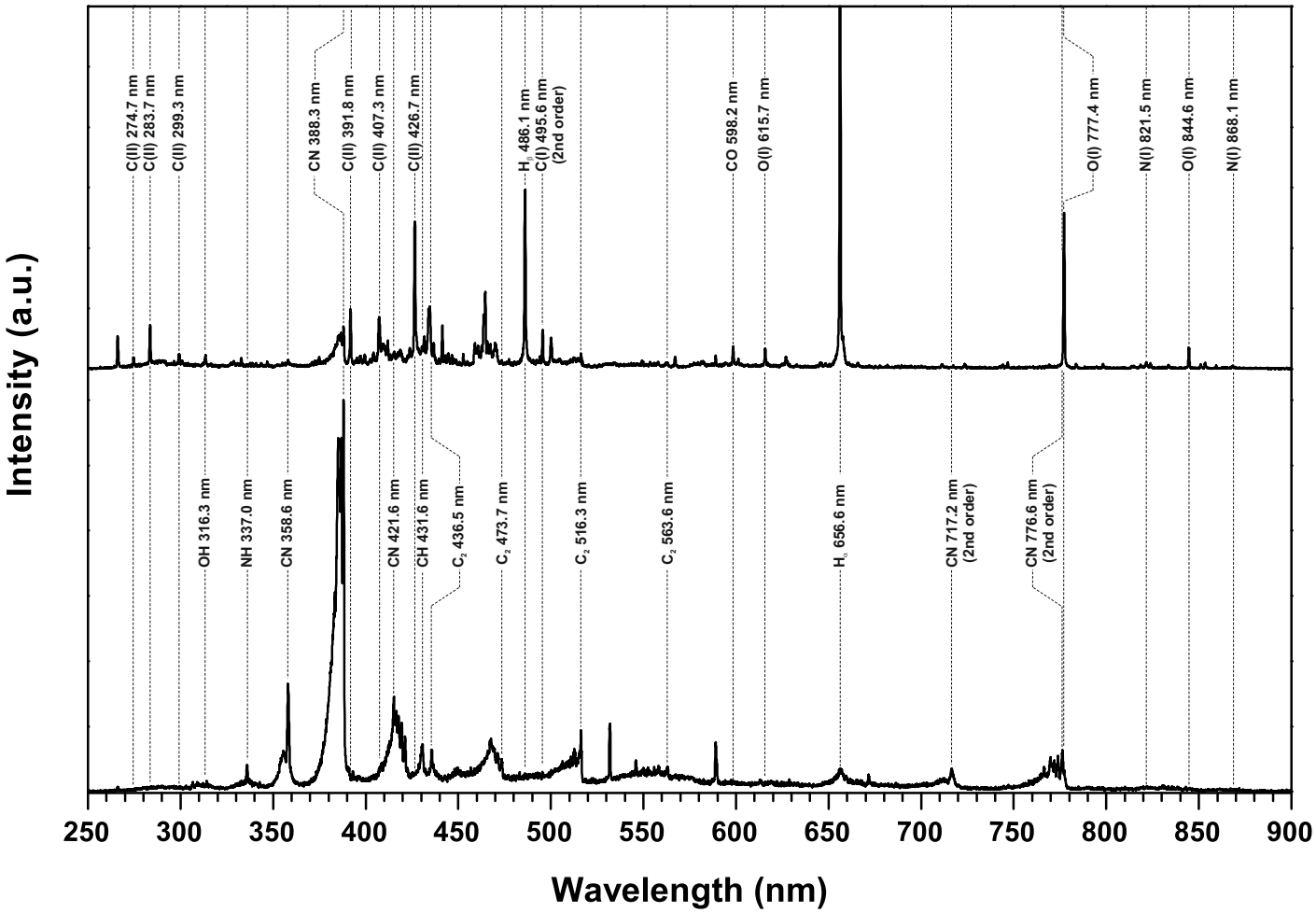

Figure 2

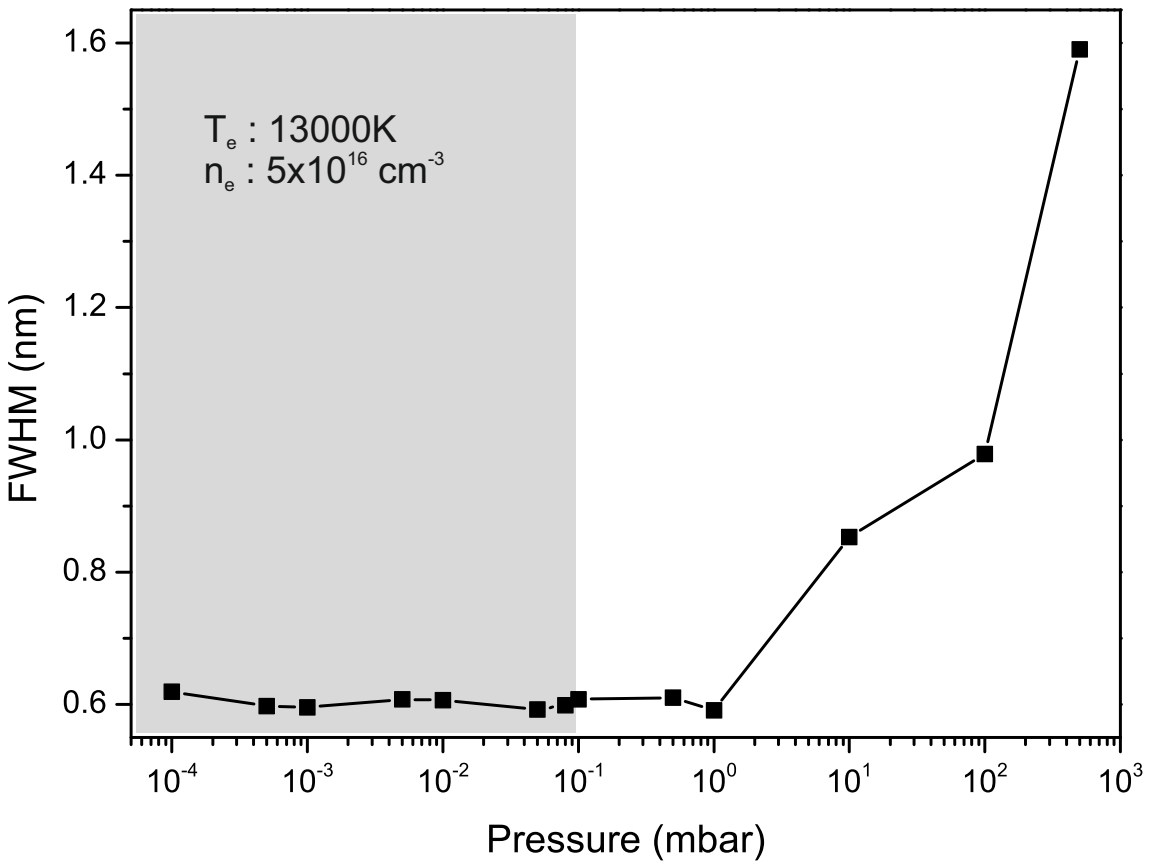

Figure 3

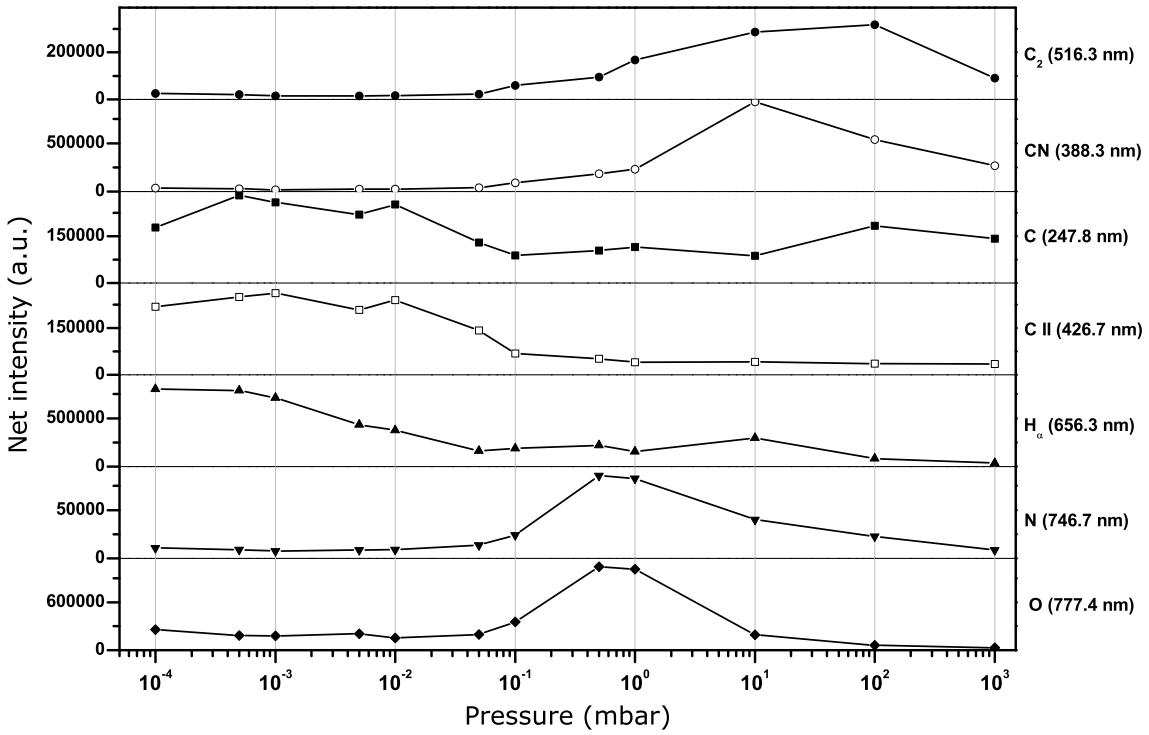

Figure 4

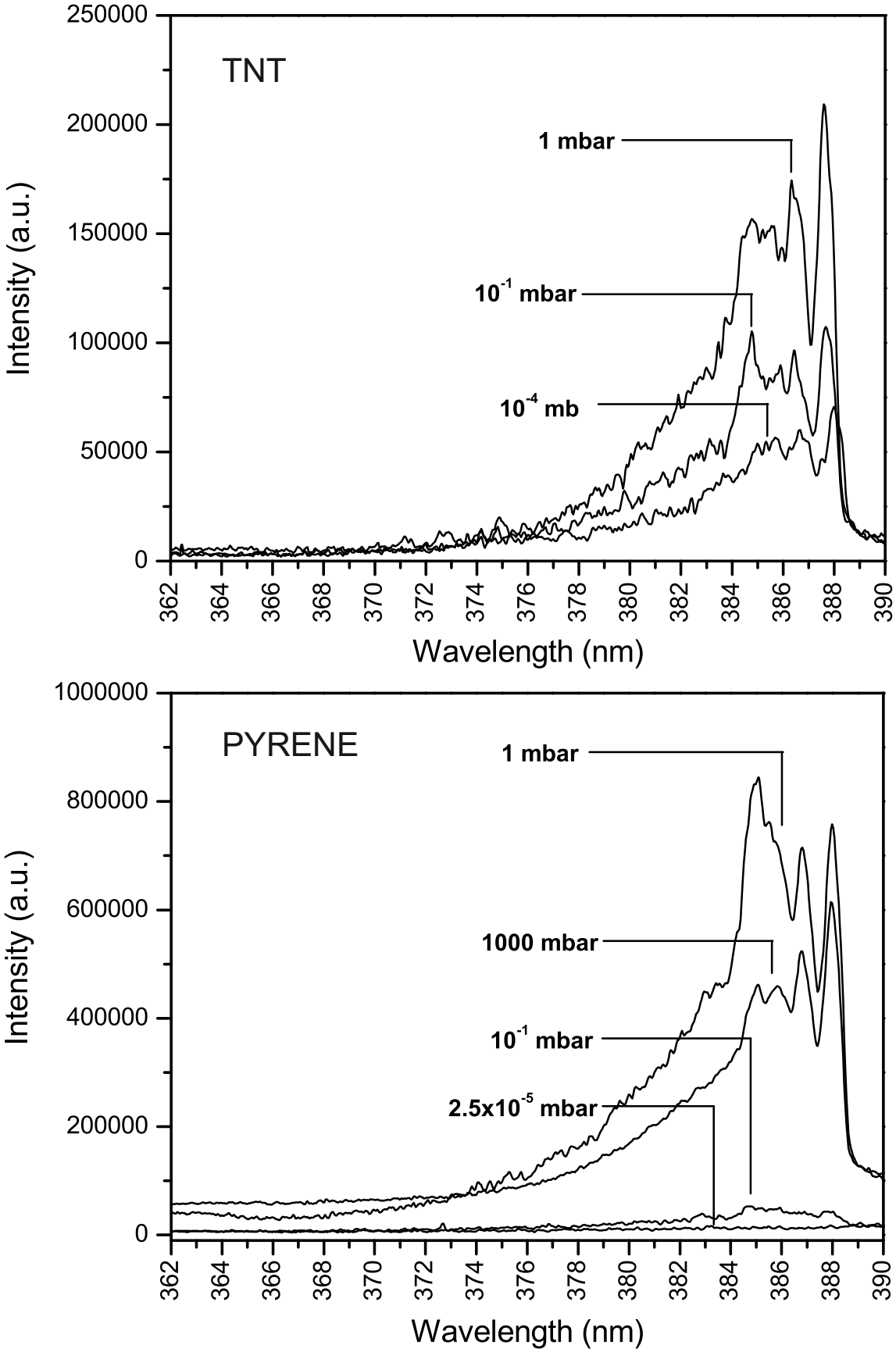

Figure 5

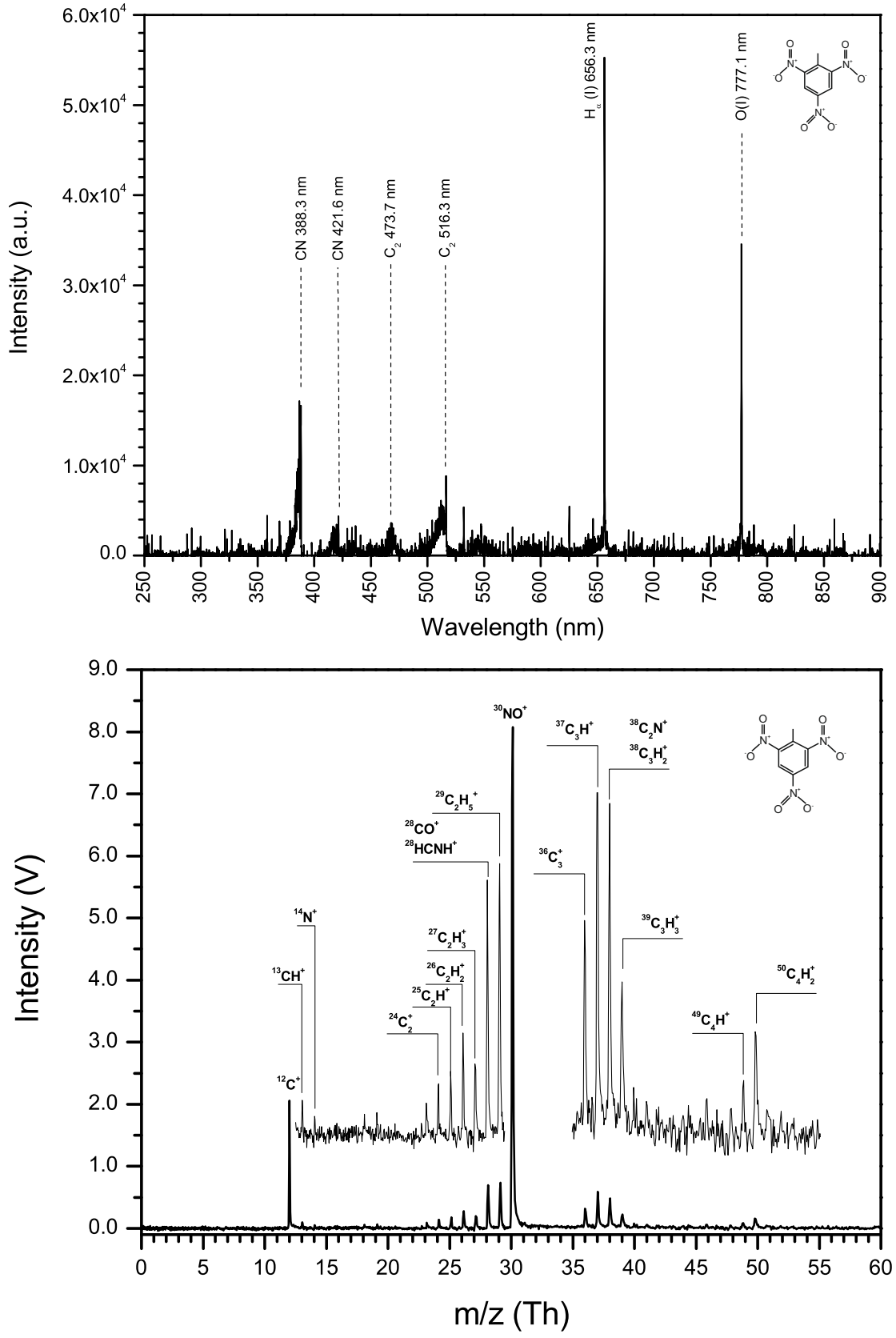

Figure 6

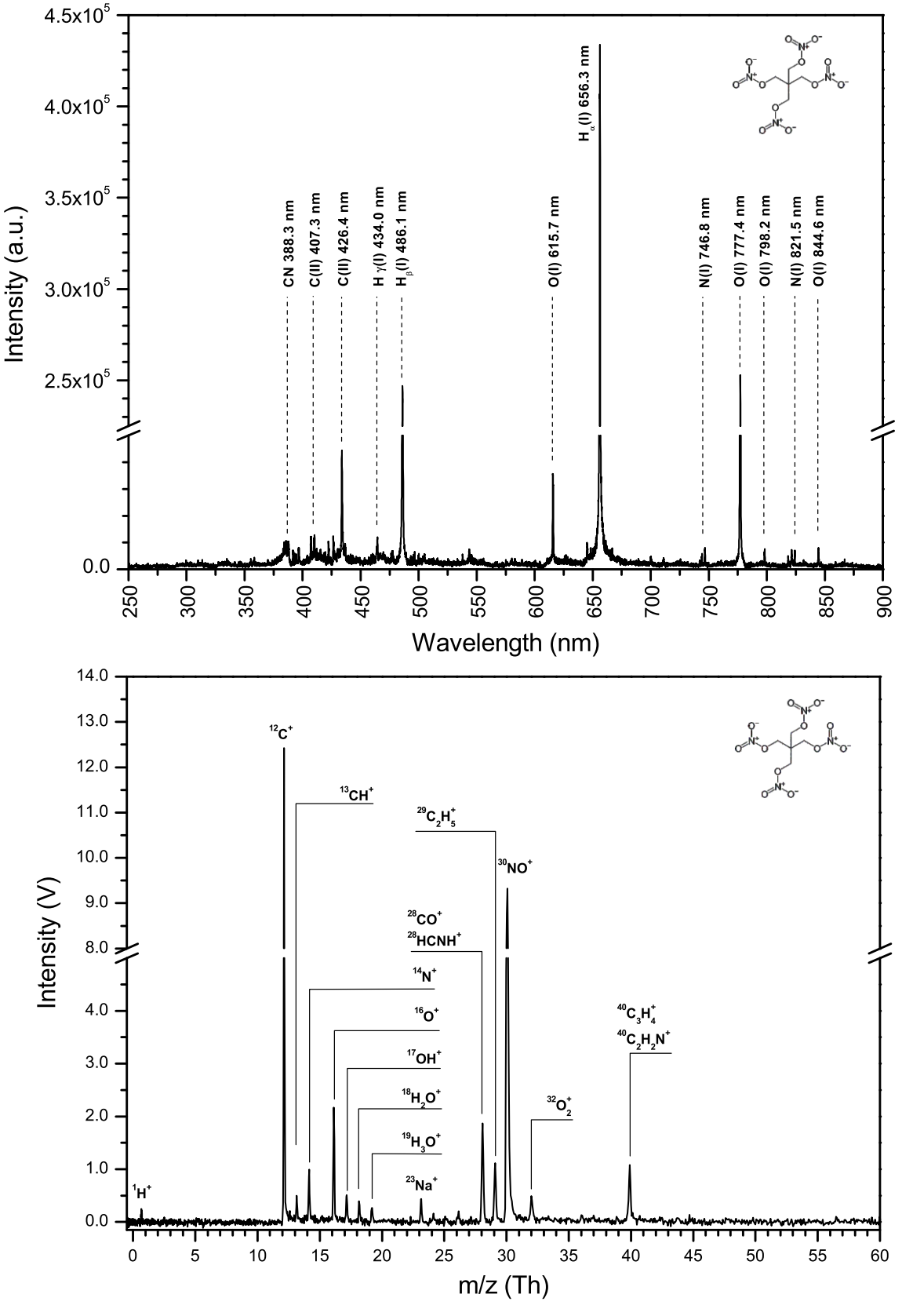

Figure 7

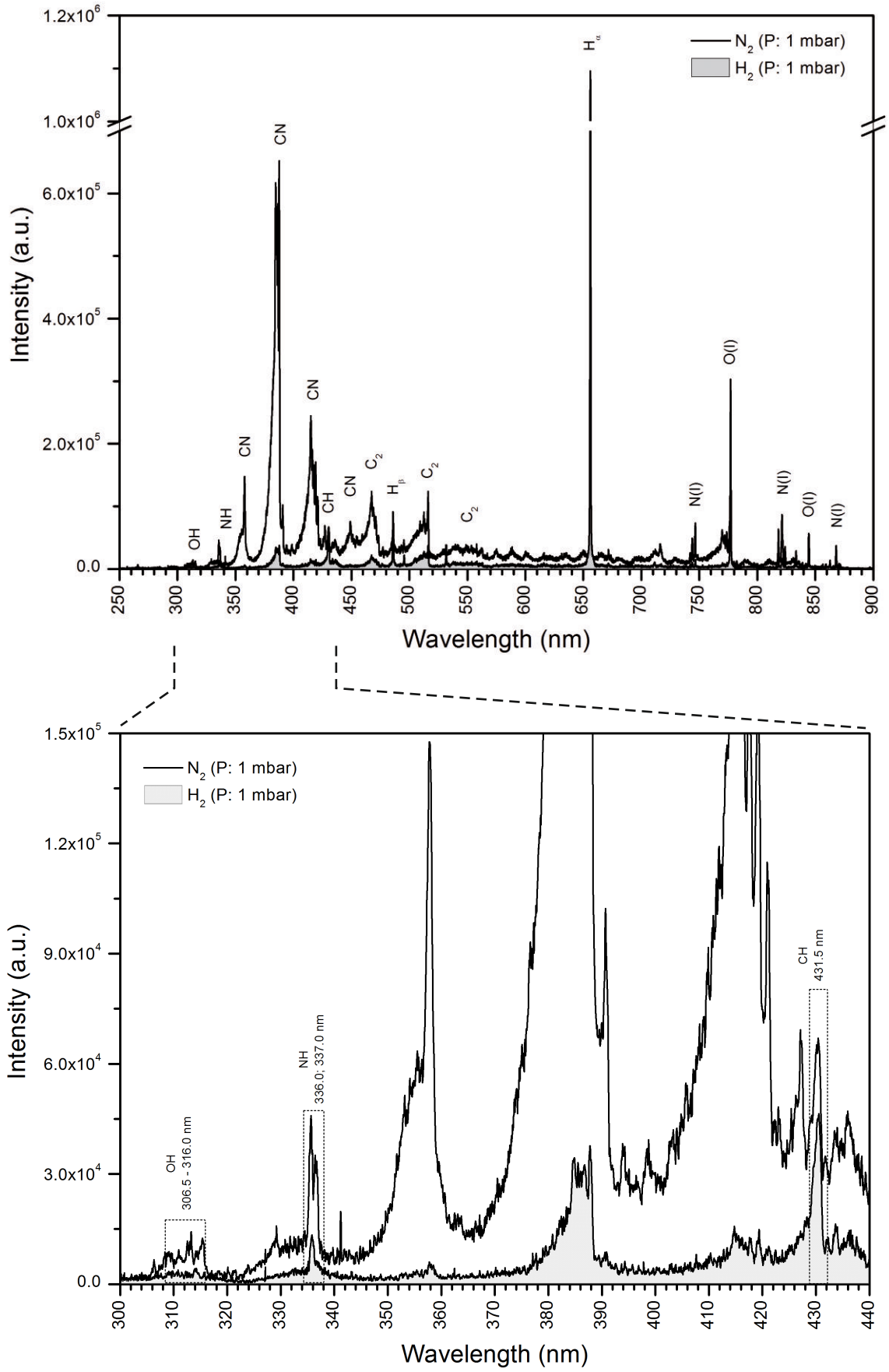

Figure 8

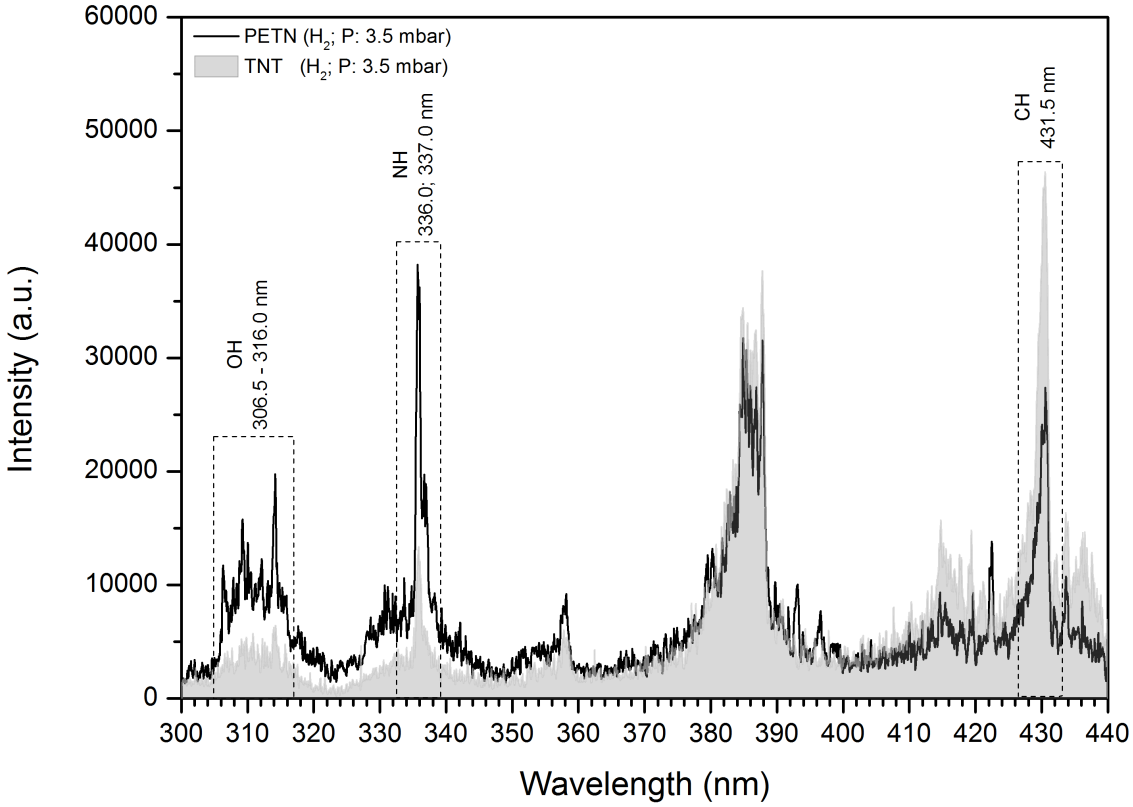

Figure 9